International Journal of Mechanical, Industrial and Aerospace Sciences
ISSN: 2517-9950
Vol:9, No:9, 2015

Dynamic Behavior of the Nanostructure of Load-bearing Biological Materials

M. Qwamizadeh, K. Zhou, Z. Zhang, YW. Zhang

***Abstract*—**Typical load-bearing biological materials like bone, mineralized tendon and shell, are biocomposites made from both organic (collagen) and inorganic (biomineral) materials. This amazing class of materials with intrinsic internally designed hierarchical structures show superior mechanical properties with regard to their weak components from which they are formed. Extensive investigations concentrating on static loading conditions have been done to study the biological materials failure. However, most of the damage and failure mechanisms in load-bearing biological materials will occur whenever their structures are exposed to dynamic loading conditions. The main question needed to be answered here is: What is the relation between the layout and architecture of the load-bearing biological materials and their dynamic behavior? In this work, a staggered model has been developed based on the structure of natural materials at nanoscale and Finite Element Analysis (FEA) has been used to study the dynamic behavior of the structure of load-bearing biological materials to answer why the staggered arrangement has been selected by nature to make the nanocomposite structure of most of the biological materials. The results showed that the staggered structures will efficiently attenuate the stress wave rather than the layered structure. Furthermore, such staggered architecture is effectively in charge of utilizing the capacity of the biostructure to resist both normal and shear loads. In this work, the geometrical parameters of the model like the thickness and aspect ratio of the mineral inclusions selected from the typical range of the experimentally observed feature sizes and layout dimensions of the biological materials such as bone and mineralized tendon. Furthermore, the numerical results validated with existing theoretical solutions. Findings of the present work emphasize on the significant effects of dynamic behavior on the natural evolution of load-bearing biological materials and can help scientists to design bioinspired materials in the laboratories.

***Keywords*—**Load-bearing biological materials, nanostructure, staggered structure, stress wave decay.

I. Introduction

BIOLOGICAL materials with extraordinary mechanical properties show different levels of structural hierarchies [1], [2]. For instance, it is reported that there exists seven levels for bone [3], around four and two structural levels for mineralized tendon [4] and shell [5], respectively. The number of hierarchical levels is very crucial in those materials because at different dimension scales, different damage and deformation mechanisms may occur [2]. It should be noted that in biological materials there is an intrinsic hierarchical architecture with regard to the different combination of organic and inorganic portions [1]-[3]. Thus, to understand how the structure and mechanical properties of these biological materials are related to each other, multi-scale modeling and simulations provide a powerful tool.

With regard to the important functionalities of load-bearing biological materials, various studies have been performed to investigate their constitution, mechanical characteristics, structures and the relationship between the intrinsic multi-level architecture and superior mechanical properties of natural materials [6]-[10].

The functionalities, structures and properties of the biological materials have been selected during natural evolution [2]. The structural dimensions and layouts of biological materials like bone and shells are naturally designed to make such structures with superior strength and exceptional fracture toughness [11]. Various analytical models have been used to study the relation between the complex structure and impressive mechanical properties of load-bearing biological materials at nanoscale [12]-[17]. Moreover, the structural feature size and dimensions of the nanostructure of biological materials have been studied experimentally [18]-[28].

In larger scales, various self-similar as well as quasi-self-similar models have been developed to study the mechanical properties of the biological structures at different length scales [29], [30]. At the same time, finite element method has been extensively performed to study the mechanical behavior of load-bearing biological materials in both single and multiple hierarchies [31]-[37]. For instance, finite element method has been used to study the failure mechanism of tropocollagen molecules attached together with nanoscale cross links [38].

It should be noted that almost all the previous analytical and numerical studies discussed here concentrated on the static analysis of the load-bearing biological materials from the standpoint of strength and fracture toughness. Meanwhile, the most significant functionality of the load-bearing biological materials like bone is to protect the soft organs from dynamic loading. As a result, the stress wave decay within the biological structure becomes critically significant. Consequently, those biological structures with faster stress wave attenuation will effectively damp the loads and efficiently protect the soft organs from impact.

In this work, finite element analysis was used to investigate the dynamic response of the nanostructure of load-bearing biological materials. To do the procedure, first of all we verify our numerical results with the results obtained for a laminated structure [39]-[44]. Then, systematic finite element analysis will be performed to investigate the dynamic response of the

M. Qwamizadeh is with Agency for Science, Technology and Research, the Institute of High Performance Computing, A*STAR, Singapore 138632, Singapore, and Ph.D candidate of the school of Mechanical and Aerospace Engineering, Nanyang Technological University, Singapore 639798, Singapore; (corresponding author: mahan001@e.ntu.edu.sg).

structure of the biological materials at nanoscale.

II. Mechanical and FEM Models

Most of the natural materials possess some common and similar features at the smallest level of their hierarchical structures. Fig. 1 shows the hierarchical architecture of the bone as one of the most complicated biostructures.

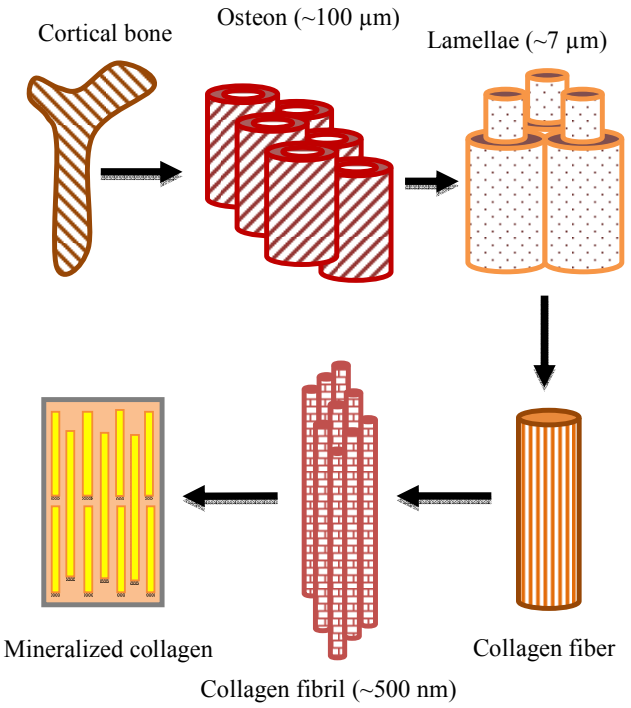

Fig. 1 Bone Structural Hierarchy

As it is seen, in the larger scales osteons which have central holes (Haversian canals) are the main building blocks of the cortical bone. In smaller length scales, lamellae (~3-7 µm) will form the collagen fibers which are formed from different collagen fibrils (~0.5 µm). Collagen fibrils are composed of collagen molecules which are triple helix with approximate length of 300 nm and diameter of 1.5 nm. Finally, by nucleating hydoxyapatite crystals within the collagen molecules, a staggered arrangement composed of mineral and protein makes the nanostructure of the bone at the smallest scale [1], [2], [45]. The nanostructure of most of the load-bearing biological materials is similar to that of the bone. This nanocomposite which is a protein matrix with embedded mineral nanocrystals is known as the mineralized collagen structure. This nanostructure has been supported by various experiments [22], [27], [28] and widely used to investigate the relation between the structure and properties of the load-bearing biological materials [13], [15], [17], [29].

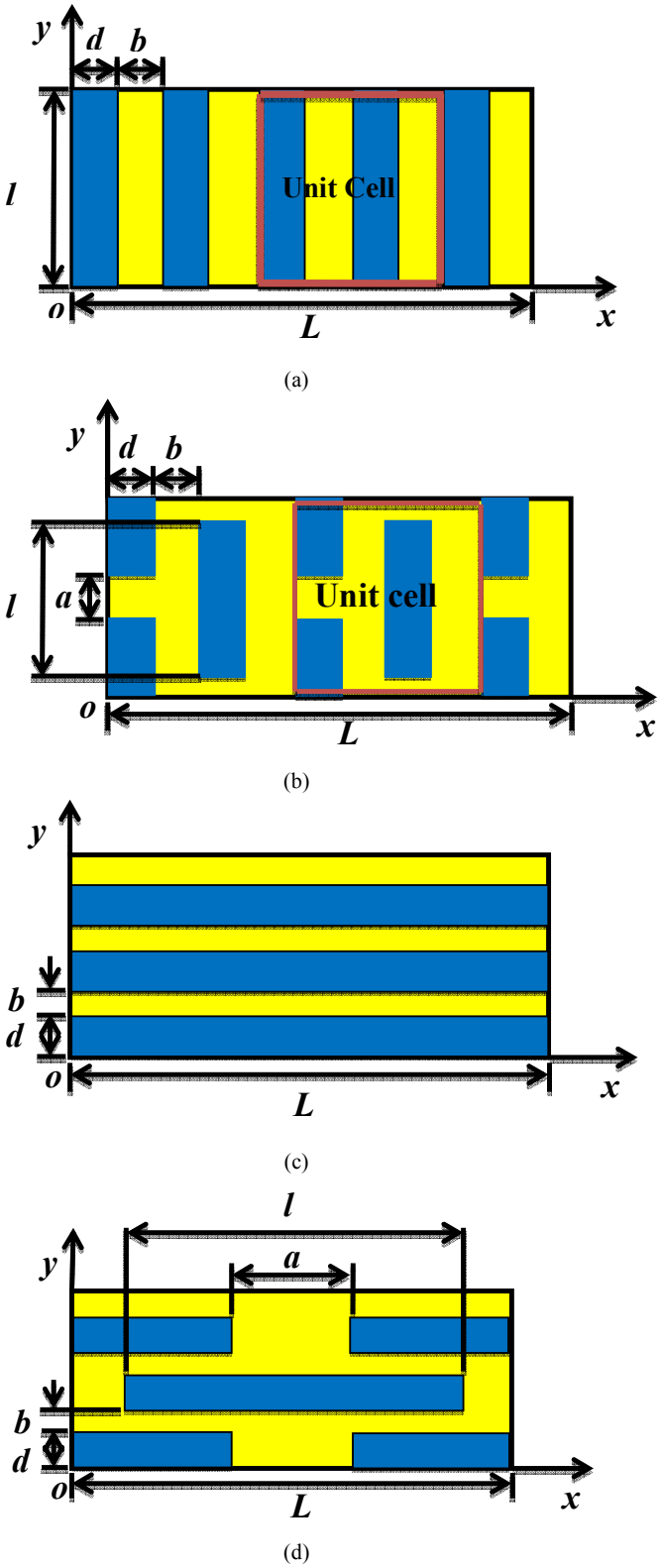

Fig. 2 Geometry of structural models: (a) vertically layered, (b) vertically staggered, (c) horizontally layered, (d) horizontally staggered structures

In the present work, we focus on the mineralized collagen structure as the primary hierarchical structure of the load-bearing biological materials to study their dynamic behavior under the impact loading condition. To do so, four different arrangements as depicted in Fig. 2 have been considered to perform the numerical analysis.

III. FEM Model Validation

Since there is no analytical approach to study the wave traveling through the staggered structure under impact loading, it is inevitable to verify our simulation results with the theoretical results of the laminated structure (refer to Fig. 2 (a)). Nonetheless, it should be noted that the theoretical solution existing for the laminated structure is only valid for the structure exposed to unit step loading. In such this condition, the stress wave traveling through the laminated structure is in the form of airy function under the step load σ_0, which is imposed on the left vertical side of the model (refer to Fig. 2 (a)), and has the form:

$$\sigma(x,t)=\sigma_0\left[\frac{1}{3}+\int_0^R Airy(-S)\,\mathrm{d}S\right] \tag{1}$$

$$R=\left(t-\frac{x}{c_0}\right)\left(\frac{2}{h'''(0)t}\right)^{1/3} \tag{2}$$

$$h'''(0)=\frac{c_0^2}{(d+b)^2}\left(\frac{d}{c_h}\right)^2\left(\frac{b}{c_s}\right)^2\left[\frac{1}{4}\left(\frac{\rho_h c_h}{\rho_s c_s}+\frac{\rho_s c_s}{\rho_h c_h}\right)^2-1\right] \tag{3}$$

where c_h and c_s are the wave speeds in the hard and the soft component, respectively; and can be calculated by:

$$c_h=\sqrt{\frac{E_h}{\rho_h}},\ c_s=\sqrt{\frac{E_s}{\rho_s}} \tag{4}$$

c_0 is the phase velocity for the laminated system and can be obtained as:

$$c_0=\frac{d+b}{\sqrt{\left(\frac{d}{c_h}\right)^2+\left(\frac{b}{c_s}\right)^2+\left(\frac{\rho_h c_h}{\rho_s c_s}+\frac{\rho_s c_s}{\rho_h c_h}\right)\frac{db}{c_h c_s}}} \tag{5}$$

E_h and ρ_h are the Young's modulus and the density of the hard layer, respectively; E_s and ρ_s are those of the soft layer as well.

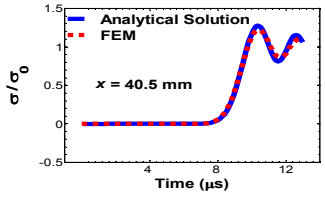

(a)

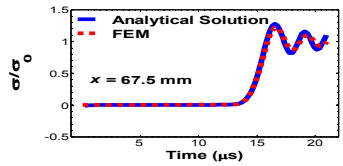

(b)

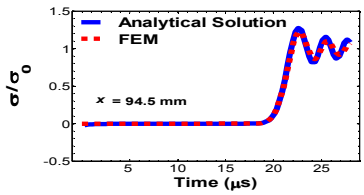

(c)

Fig. 3 Comparison of stress wave profiles obtained from FEM with those calculated from theoretical work [39] for (a) x = 40.5 mm, (b) x = 67.5 mm, (c) x = 94.5 mm (d = 1.5 mm, b = 1.2 mm, E_h = 108 GPa, E_s = 2025 GPa, ρ_h = 3 g/cm^3, ρ_s = 0.25 g/cm^3)

Fig. 3 compares the wave profiles within the vertically layered arrangement in different distances from the origin of the structure in both analytical and FEM solutions. In this condition, the wave profile starts vanishing after passing some distances for each time step. For the small time, the stress will decrease fast and for the large time steps the stress will start decreasing after passing a long distance. It is obvious that there is more time delay for wave profile when the distance is increased. It means that the wave needs more time to reach the particular position traveling through the media. It is shown that the results obtained by the present simulation became compatible with those obtained from analytical solution for the wave front. In our FEM simulations, the degrees of freedom of the model along the right boundary are fixed in all the directions, and those at the top and the bottom boundary are fixed only along the vertical direction. As it is seen in Fig. 3, there exists an excellent consistency between the analytical and simulation results for the wave front but beyond that both solutions tend to deviate from each other. This is due to the fact that the theoretical solution [39] here is naturally an asymptotic solution and its results are only valid for the wave front. Since the theoretical results are not valid for the whole domain and with regard to the excellent compatibility of the FEM and analytical results for the wave front, one can readily find that FEM results will make a trustable solution for the stress wave through the whole traveling domain.

Before starting the simulation for the staggered biomaterial, there is need to investigate the effect of the element numbers and homogenous as well as non-homogeneous mesh on the results obtained by numerical simulation to ensure the correct convergence of the solution. For this purpose, the number of the elements in the model was increased to investigate the mesh dependency of the model. Also a homogeneous mesh was generated on the model to study the effect of using fine mesh on the stress.

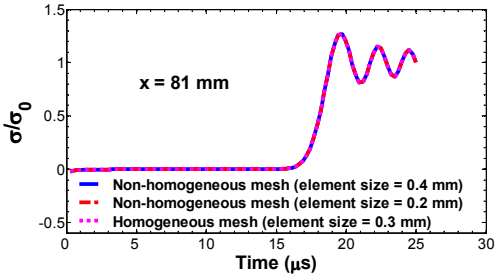

(a)

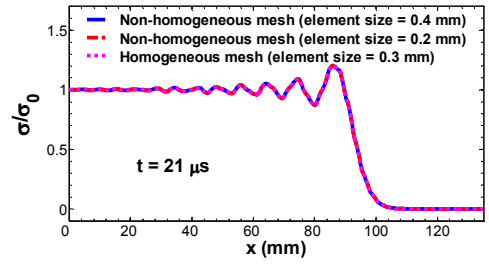

(b)

Fig. 4 The wave profile passing through the layered composite (a) versus time, (b) versus distance for different element sizes ($d = 1.5$ mm, $b = 1.2$ mm, $E_h = 108$ GPa, $E_s = 20.25$ GPa, $\rho_h = 3$ g/cm^3, $\rho_s = 0.25$ g/cm^3)

TABLE I
COMPARISON OF THE WAVE VELOCITIES IN DIFFERENT ELEMENT SIZES CALCULATED BY FEM WITH THAT OBTAINED FROM ANALYTICAL SOLUTION

Mesh size	c_0 (mm/s)	c_0 calculated from analytical solution (mm/s)
1.0 mm	4.70423×10^6	4.5566×10^6
0.8 mm	4.70361×10^6	
0.6 mm	4.70339×10^6	
0.4 mm	4.70327×10^6	
0.2 mm	4.70318×10^6	
0.1 mm	4.70313×10^6	

($d = 1.5$ mm, $b = 1.2$ mm, $E_h = 108$ GPa, $E_s = 20.25$ GPa, $\rho_h = 3$ g/cm^3, $\rho_s = 0.25$ g/cm^3)

Table I shows the wave velocities obtained from our FEM simulations using different element sizes. It is seen that the FEM results at different element sizes are nearly the same, indicating the convergence of the finite element discretization. However, the calculated values are slightly higher than the theoretical one. It should be noted that this difference arise from the fact that c_0 is the phase velocity which is obtained from dispersion relation and it should be noted that (5) is obtained by letting time tend to infinity, which means that it is valid only for a large propagation distance.

IV. Result Analysis

Up to now it is shown that the numerical solution is reliable by verifying the FEM model with the analytical results of the laminated structure. Now it is possible to switch the model to the staggered arrangement which has been used for nanostructure of most of the load-bearing biological materials through the millions of years of biological evolution. To do so, we start from a layered unit cell (refer to Fig. 2 (a)). The mineral volume fraction of the layered structure can be obtained as:

$$\phi = \frac{d}{b+d} \tag{6}$$

By switching the layered unit cell to the staggered unit cell (refer to Fig. 2 (b)), one can easily find the mineral volume fraction of staggered structure as following:

$$\phi = \frac{ld}{(l+a)(b+d)} \tag{7}$$

All the geometrical parameters shown in Fig. 2 can be obtained from (6) and (7) for layered and staggered structures. The objective here is to compare the dynamic response of the layered and staggered nanostructures. For a better comparison we assume that the mineral volume fraction as well as the unit cell area is considered to be constant for both the layered and staggered arrangements. The mineral volume fraction ratio of most of the biological materials is known at macroscale levels. For example, for bone it is reported to be in the range of 30-48%, for mineralized tendon it is around 15% and for sea shells and nacre very large amounts of mineral volume fraction around 95% have been reported [5], [13], [46]. In this work, bone as a typical load-bearing biological material has been taken into account. Regarding to the hierarchical structure of the bone, it is expected that mineral volume fraction in smaller length scales is to be greater than that of the macroscale but the mineral volume fraction in the nanostructure of biological materials is still unknown. However, several experiments have been performed to measure the structural dimensions of the mineral plates nucleated in the collagen matrix at nanoscale [18], [21], [23]-[28]. The axial period of the tropocollagen molecules in the staggered unmineralized collagen structure is suggested to be around 67 nm which contains gap and overlapping regions [2], [45]. By nucleating the hydroxyapatite crystals within the gap regions of the collagen matrix, the mineralized collagen structure of the biological materials at nanoscale can be created [1], [2], [45]. The experimental results revealed the geometrical ranges for the structural parameters of the bone nanostructure. For instance, it was reported that the thickness of the mineral plates is about 2-10 nm while their length is reported to be up to150 nm [28], [47]. It was also reported that the distance between the mineral platelets is about 2-4.5 nm [46].

To calculate the geometrical parameters we start from the layered structure with typical structural dimensions within the experimental range. Then by calculating the mineral volume fraction and the unit cell area of the layered arrangement, the dynamic response of the layered arrangement can be studied. To analyze the staggered arrangement, by fixing the mineral volume fraction and unit cell area to the same values obtained

for layered structure and changing the mineral plate thickness, different staggered structure with same volume fraction and unit cell area can be provided. Consequently, comparative studies between the layered and different staggered structures will be done to investigate their dynamic behavior.

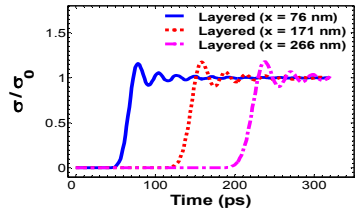

(a)

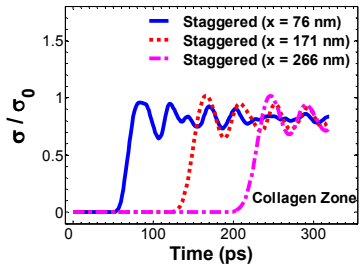

(b)

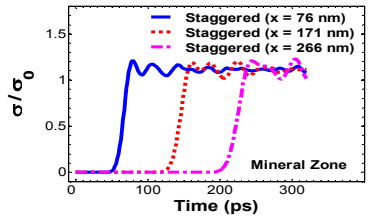

(c)

Fig. 5 Wave profiles passing through the vertically (a) layered structure, (b) staggered structure at the middle of the collagen zone, (c) staggered structure at the middle of the mineral zone ($d = 4$ nm, $b = 5.5$ nm, $E_m = 130$ GPa, $E_c = 1$ GPa, $\nu_m = \nu_c = 0.28$, $\rho_m = 2$ g/cm^3, $\rho_c = 1$ g/cm^3)

Fig. 5 compares the wave profile passing through the vertically layered and staggered structures in different distances from the origin of the structure. For the staggered arrangement, the wave profiles are plotted for both the soft collagen and hard mineral counterparts. As it is shown, the wave profile in the layered structure does not change in different distances from the origin of the structure. Meanwhile, the passing time will be changed that means for distances far from the impact surface, the wave needs more time to reach to that position as well. However, the significant difference between the wave profiles in the hard and soft portion of the staggered structure is obvious for different distances from the origin of the structure. As it is expected, the stress values in the collagen (soft portion) are less than those of the mineral (hard) one.

To compare the dynamic response of the layered and staggered nanostructures, we impose an impact load in the left vertical side (x = 0) of the models shown in Fig. 2. Then by extracting the stress results of all the elements of the unit cells, and by calculating the area of the elements based on the coordinates of each element within the unit cell, the average stress for each unit cell can be calculated.

Fig. 6 shows the plot of the average normal stress versus dimensionless model length for the vertically layered and staggered structures. It should be noted that in all the layered and staggered cases studied here the mineral volume fraction and unit cell area are considered to be the same for consistency. The results showed that the average normal stress in the layered structure is greater than that in the staggered structures. This means that the staggered architectures are efficiently damp the stress wave rather than the laminated structures. It can provide a convincing explanation that why nature selects staggered layouts rather than the laminated structure for the nanostructure of the load-bearing biological materials.

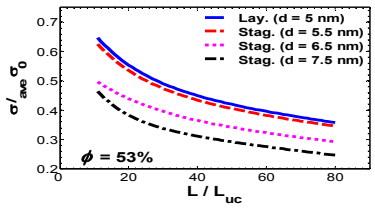

(a)

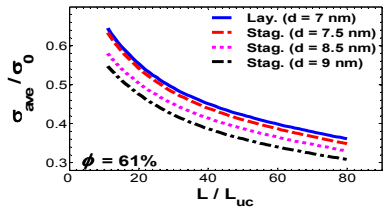

(b)

Fig. 6 Average stress wave attenuation within the vertically layered and staggered structures for mineral volume fraction of (a) 53%, (b) 61% ($E_m = 130$ GPa, $E_c = 1$ GPa, $\nu_m = \nu_c = 0.28$, $\rho_m = 2$ g/cm^3, $\rho_c = 1$ g/cm^3)

Fig. 7 shows the average normal stress wave attenuation for the horizontally layered and staggered structures for two typical volume fraction ratios. As it is seen, the results again show that the average normal stress in the staggered structures is less than that of the laminated one. It emphasize that the staggered structures are able to attenuate the stress wave faster than the laminated layout. Regarding the main functionality of the load-bearing biological materials which is protecting the inside organs from dynamic impact, staggered structures has shown to be better choices to carry out this functionality.

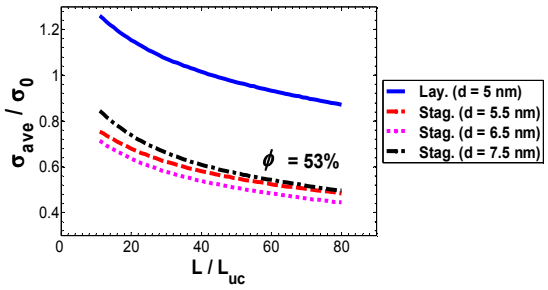

(a)

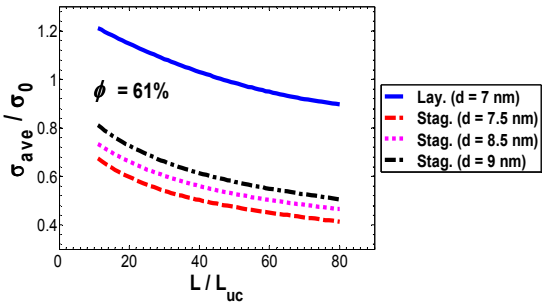

(b)

Fig. 7 Average stress wave attenuation within the horizontally layered and staggered structures for mineral volume fraction of (a) 53%, (b) 61% ($E_m = 130$ GPa, $E_c = 1$ GPa, $\nu_m = \nu_c = 0.28$, $\rho_m = 2$ g/cm^3, $\rho_c = 1$ g/cm^3)

In Fig. 8 we compared the average normal as well as shear stress in both vertically and horizontally layered and staggered arrangements. As it is seen for vertically arrangements in Figs. 8 (a), (b), the average normal stress in staggered structures are less than that of the laminated architecture. On the other hand, the laminated structure shows very small shear stress which is approximately near zero. Meanwhile, the staggered structures show moderate values for both normal and shear stresses which means that the staggered arrangement is efficiently acting in utilizing the capacity to resist both normal and shear stresses with regard to the fact that both collagen and mineral have specific capacity in resisting normal and shear stresses. This could be another convincing explanation that why the staggered layout will be naturally selected for the structure of most of the biological materials at nanoscale. The same results can be seen for the horizontally layered and staggered arrangements in Figs. 2 (c), (d).

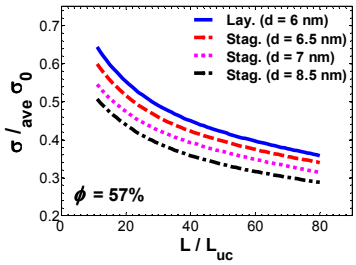

(a)

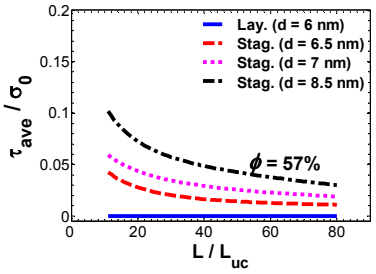

(b)

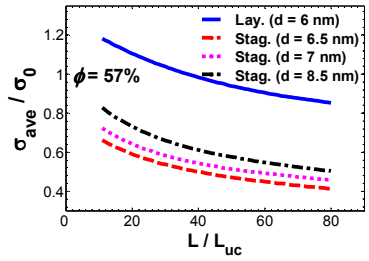

(c)

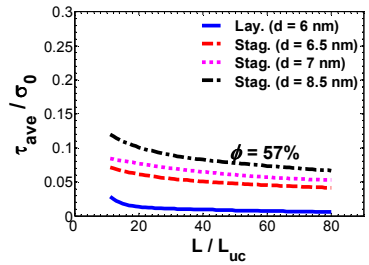

(d)

Fig. 8 Comparison of average (a) normal, (b) shear stress in vertically layered and staggered structure and comparison of average (c) normal, (d) shear stress in horizontally layered and staggered structure for mineral volume fraction of 57% ($E_m = 130$ GPa, $E_c = 1$ GPa, $\nu_m = \nu_c = 0.28$, $\rho_m = 2$ g/cm^3, $\rho_c = 1$ g/cm^3)

V. Conclusion

We performed systematic finite element analysis to study the dynamic response of the structure of load-bearing biological materials at their first hierarchical level. Both the laminated and staggered nanostructures have been taken into account during the numerical analysis. The simulation results showed that the staggered structure can damp the stress wave faster than the laminated structure with the same mineral volume fraction and unit cell area. Moreover, the average normal stress in the staggered arrangement is smaller than that of the layered structure; meanwhile, the shear stress in the staggered structure is larger than that in the laminated one which is the cost of the decrease in normal stress of the staggered structures. Regarding the fact that collagen and mineral can resist both tensile and shear stress, the staggered arrangement can utilize its capacity to resist both tensile and shear stress; however, the layered arrangement cannot

effectively use its capacity to resist shear loading. Interestingly, the present work findings will provide a cogent explanation that why the nanostructure of most of the biological materials have been compatible with the staggered architecture at their primary hierarchical levels during the natural evolution.

ACKNOWLEDGMENT

M. Qwamizadeh thanks Agency for Science, Technology and Research (A*STAR) and Singapore International Graduate Award (SINGA) for providing his PhD scholarship.

REFERENCES

[1] J. Y. Rho, L. Kuhn Spearing, and P. Zioupos, "Mechanical properties and the hierarchical structure of bone," *Medical engineering & physics,* vol. 20, pp. 92-102, 1998.
[2] M. A. Meyers, P. Y. Chen, A. Y. M. Lin, and Y. Seki, "Biological materials: structure and mechanical properties," *Progress in Materials Science,* vol. 53, pp. 1-206, 2008.
[3] S. Weiner and H. D. Wagner, "The material bone: structure-mechanical function relations," *Annual Review of Materials Science,* vol. 28, pp. 271-298, 1998.
[4] R. Puxkandl, I. Zizak, O. Paris, J. Keckes, W. Tesch, S. Bernstorff, *et al.*, "Viscoelastic properties of collagen: synchrotron radiation investigations and structural model," *Philosophical Transactions of the Royal Society of London. Series B: Biological Sciences,* vol. 357, pp. 191-197, 2002.
[5] R. Menig, M. Meyers, M. Meyers, and K. Vecchio, "Quasi-static and dynamic mechanical response of *Strombus gigas* (conch) shells," *Materials Science and Engineering: A,* vol. 297, pp. 203-211, 2001.
[6] J. D. Currey, *The mechanical adaptations of bones*. Princeton: Princeton University Press, 1984.
[7] P. D. Delmas, R. P. Tracy, B. L. Riggs, and K. G. Mann, "Identification of the noncollagenous proteins of bovine bone by two-dimensional gel electrophoresis," *Calcified tissue international,* vol. 36, pp. 308-316, 1984.
[8] P. Fratzl and R. Weinkamer, "Nature's hierarchical materials," *Progress in Materials Science,* vol. 52, pp. 1263-1334, 2007.
[9] H. D. Espinosa, J. E. Rim, F. Barthelat, and M. J. Buehler, "Merger of structure and material in nacre and bone perspectives on *de novo* biomimetic materials," *Progress in Materials Science,* vol. 54, pp. 1059-1100, 2009.
[10] R. O. Ritchie, "The conflicts between strength and toughness," *Nature Materials,* vol. 10, pp. 817-822, 2011.
[11] Y. Shao, H.-P. Zhao, and X.-Q. Feng, "On flaw tolerance of nacre: a theoretical study," *Journal of The Royal Society Interface,* vol. 11, p. 20131016, 2014.
[12] H. Gao, B. Ji, I. L. Jäger, E. Arzt, and P. Fratzl, "Materials become insensitive to flaws at nanoscale: lessons from nature," *Proceedings of the national Academy of Sciences,* vol. 100, pp. 5597-5600, 2003.
[13] B. Ji and H. Gao, "Mechanical properties of nanostructure of biological materials," *Journal of the Mechanics and Physics of Solids,* vol. 52, pp. 1963-1990, 2004.
[14] B. Ji and H. Gao, "A study of fracture mechanisms in biological nano-composites via the virtual internal bond model," *Materials Science and Engineering: A,* vol. 366, pp. 96-103, 2004.
[15] B. Ji, H. Gao, and K. Jimmy Hsia, "How do slender mineral crystals resist buckling in biological materials?," *Philosophical Magazine Letters,* vol. 84, pp. 631-641, 2004.
[16] B. Ji, H. Gao, and T. Wang, "Flow stress of biomorphous metal–matrix composites," *Materials Science and Engineering: A,* vol. 386, pp. 435-441, 2004.
[17] B. Ji and H. Gao, "Elastic properties of nanocomposite structure of bone," *Composites science and technology,* vol. 66, pp. 1212-1218, 2006.
[18] R. A. Robinson, "An electron-microscopic study of the crystalline inorganic component of bone and its relationship to the organic matrix," *The Journal of Bone & Joint Surgery,* vol. 34, pp. 389-476, 1952.
[19] R. A. Robinson and M. L. Watson, "Collagen-crystal relationships in bone as seen in the electron microscope," *The anatomical record,* vol. 114, pp. 383-409, 1952.
[20] R. A. Robinson and M. L. Watson, "Crystal-collagen relationships in bone as observed in the electron microscope. III. Crystal and collagen morphology as a function of age," *Annals of the New York Academy of Sciences,* vol. 60, pp. 596-630, 1955.
[21] Z. Molnar, "Additional observations on bone crystal dimensions," *Clin. Orthop,* vol. 17, pp. 38-42, 1960.
[22] A. S. Posner, "Crystal chemistry of bone mineral," *Physiological reviews,* vol. 49, pp. 760-792, 1969.
[23] J. Moradian-Oldak, S. Weiner, L. Addadi, W. Landis, and W. Traub, "Electron imaging and diffraction study of individual crystals of bone, mineralized tendon and synthetic carbonate apatite," *Connective tissue research,* vol. 25, pp. 219-228, 1991.
[24] W. Landis, M. Song, A. Leith, L. McEwen, and B. McEwen, "Mineral and organic matrix interaction in normally calcifying tendon visualized in three dimensions by high-voltage electron microscopic tomography and graphic image reconstruction," *Journal of structural biology,* vol. 110, pp. 39-54, 1993.
[25] V. Ziv and S. Weiner, "Bone crystal sizes: a comparison of transmission electron microscopic and X-ray diffraction line width broadening techniques," *Connective tissue research,* vol. 30, pp. 165-175, 1994.
[26] W. Landis, "The strength of a calcified tissue depends in part on the molecular structure and organization of its constituent mineral crystals in their organic matrix," *Bone,* vol. 16, pp. 533-544, 1995.
[27] M. A. Rubin, I. Jasiuk, J. Taylor, J. Rubin, T. Ganey, and R. P. Apkarian, "TEM analysis of the nanostructure of normal and osteoporotic human trabecular bone," *Bone,* vol. 33, pp. 270-282, 2003.
[28] T. Hassenkam, G. E. Fantner, J. A. Cutroni, J. C. Weaver, D. E. Morse, and P. K. Hansma, "High-resolution AFM imaging of intact and fractured trabecular bone," *Bone,* vol. 35, pp. 4-10, 2004.
[29] H. Gao, "Application of fracture mechanics concepts to hierarchical biomechanics of bone and bone-like materials," *International Journal of Fracture,* vol. 138, pp. 101-137, 2006.
[30] Z. Zhang, Y. W. Zhang, and H. Gao, "On optimal hierarchy of load-bearing biological materials," *Proceedings of the Royal Society B: Biological Sciences,* vol. 278, pp. 519-525, 2011.
[31] B. Borah, G. J. Gross, T. E. Dufresne, T. S. Smith, M. D. Cockman, P. A. Chmielewski, *et al.*, "Three-dimensional microimaging (MRμI and μCT), finite element modeling, and rapid prototyping provide unique insights into bone architecture in osteoporosis," *The anatomical record,* vol. 265, pp. 101-110, 2001.
[32] H. Gong, M. Zhang, L. Qin, and Y. Hou, "Regional variations in the apparent and tissue-level mechanical parameters of vertebral trabecular bone with aging using micro-finite element analysis," *Annals of biomedical engineering,* vol. 35, pp. 1622-1631, 2007.
[33] X. N. Dong, T. Guda, H. R. Millwater, and X. Wang, "Probabilistic failure analysis of bone using a finite element model of mineral–collagen composites," *Journal of biomechanics,* vol. 42, pp. 202-209, 2009.
[34] Q. Luo, R. Nakade, X. Dong, Q. Rong, and X. Wang, "Effect of mineral–collagen interfacial behavior on the microdamage progression in bone using a probabilistic cohesive finite element model," *Journal of the mechanical behavior of biomedical materials,* vol. 4, pp. 943-952, 2011.
[35] F. Yuan, S. R. Stock, D. R. Haeffner, J. D. Almer, D. C. Dunand, and L. C. Brinson, "A new model to simulate the elastic properties of mineralized collagen fibril," *Biomechanics and Modeling in Mechanobiology,* vol. 10, pp. 147-160, 2011.
[36] T. J. Vaughan, C. T. McCarthy, and L. M. McNamara, "A three-scale finite element investigation into the effects of tissue mineralisation and lamellar organisation in human cortical and trabecular bone," *Journal of the Mechanical Behavior of Biomedical Materials,* vol. 12, pp. 50-62, 2012.
[37] A. Barkaoui and R. Hambli, "Nanomechanical properties of mineralised collagen microfibrils based on finite elements method: biomechanical role of cross-links," *Computer methods in biomechanics and biomedical engineering,* vol. 17, pp. 1590-1601, 2014.
[38] A. Barkaoui and R. Hambli, "Finite element 3D modeling of mechanical behavior of mineralized collagen microfibrils," *Journal of Applied Biomaterials and Biomechanics,* vol. 9, pp. 199-205, 2011.
[39] C. C. Chen and R. Clifton, "Asymptotic solutions for wave propagation in elastic and viscoelastic bilaminates," in *Midwestern Mechanics Conference, 14 th, Norman, Okla*, 1975, pp. 399-417.

[40] Y. Oved, G. E. Luttwak, and Z. Rosenberg, "Shock wave propagation in layered composites," *Journal of Composite Materials,* vol. 12, pp. 84-96, 1978.
[41] N. Chandra, C. Xianglei, and A. Rajendran, "The effect of material heterogeneity on the shock response of layered systems in plate impact tests," *Journal of composites technology & research,* vol. 24, pp. 232-238, 2002.
[42] S. Zhuang, G. Ravichandran, and D. E. Grady, "An experimental investigation of shock wave propagation in periodically layered composites," *Journal of the Mechanics and Physics of Solids,* vol. 51, pp. 245-265, 2003.
[43] X. Chen and N. Chandra, "The effect of heterogeneity on plane wave propagation through layered composites," *Composites science and technology,* vol. 64, pp. 1477-1493, 2004.
[44] X. Chen, N. Chandra, and A. Rajendran, "Analytical solution to the plate impact problem of layered heterogeneous material systems," *International Journal of Solids and Structures,* vol. 41, pp. 4635-4659, 2004.
[45] I. Jäger and P. Fratzl, "Mineralized collagen fibrils: a mechanical model with a staggered arrangement of mineral particles," *Biophysical Journal,* vol. 79, pp. 1737-1746, 2000.
[46] H. A. Lowenstam and S. Weiner, *On biomineralization*. Oxford: Oxford University Press, 1989.
[47] S. J. Eppell, W. Tong, J. L. Katz, L. Kuhn, and M. J. Glimcher, "Shape and size of isolated bone mineralites measured using atomic force microscopy," *Journal of orthopaedic research,* vol. 19, pp. 1027-1034, 2001.